Lateral-Current-Injection Distributed Feedback Laser With Surface Grating Structure

Takahiko Shindo, *Student Member, IEEE*, Tadashi Okumura, *Member, IEEE*, Hitomi Ito, Takayuki Koguchi, Daisuke Takahashi, *Student Member, IEEE*, Yuki Atsumi, *Student Member, IEEE*, Joonhyun Kang, Ryo Osabe, Tomohiro Amemiya, *Member, IEEE*, Nobuhiko Nishiyama, *Senior Member, IEEE*, and Shigehisa Arai, *Fellow, IEEE*

***Abstract*—As a step toward the realization of injection-type membrane distributed feedback (DFB) lasers, which are expected to be important components of optical interconnections, we realized lateral-current-injection DFB (LCI-DFB) lasers with surface grating structures prepared on semiinsulating InP substrates. First, we designed the surface grating structure to have a high index-coupling coefficient together with a high optical confinement in the quantum wells. Then, we investigated the surface grating structure formed on an amorphous-Si (a-Si) layer deposited on the GaInAsP/InP initial wafer containing five quantum wells. A moderately low threshold current of 7.0 mA and a high differential quantum efficiency of 43% from the front facet were obtained under a continuous-wave operating condition at room temperature for a uniform grating LCI-DFB laser with a stripe width of 2.0 μm and a cavity length of 300 μm. A threshold current of 5.8 mA was obtained with a λ/4 phase-shifted LCI-DFB laser with a-Si surface grating. Furthermore, a small-signal modulation bandwidth of 4.8 GHz was obtained at a bias current of 30 mA with a modulation current efficiency factor of 1.0 GHz/mA$^{1/2}$.**

***Index Terms*—Lateral-current-injection (LCI), membrane laser, organometallic vapor phase epitaxy (OMVPE) regrowth.**

I. Introduction

THE progress in the processing speed and integration of large-scale integrated circuits (LSI) has obeyed Moore's law. However, as scaling advances, this progress will soon confront limitations associated with RC delay or ohmic heating in the electrical interconnections [1], [2]. This is especially true in global wiring, which involves relatively long-distance interconnections in the LSI; the signal-delay or the large-power dissipation will limit the performance of the LSI. Consequently, various approaches for solving these problems have been extensively studied [3]. One of the promising approaches is replacing the global wiring in the LSI with optical interconnections [4]–[6]. Optical communication played a key role in the long-distance fiber communication technology of past decades, but it is now being introduced to applications involving short-distance transmission (e.g., the explosive spread of FTTH or the introduction of optical interconnections to large-scale server systems). As a replacement for electrical wiring, optical interconnections are being extensively studied for board-to-board, chip-to-chip, and on-chip interconnections. Optical signal transmission has an advantage in terms of signal delay because it is independent of the wiring capacity. In addition, high-speed and wideband data transmission is expected from the wavelength division multiplexing technique [7]. The power dissipation of optical devices for on-chip interconnections should be much lower than that of the conventional optical components used for long-haul transmissions. For example, the available power dissipation of modulating the signal is estimated by Miller to be less than 100 fJ/bit [8]. If we want to use directly modulated semiconductor lasers, this simply means that the available injection current is limited to 1 mA when the driving voltage and modulated speed of the semiconductor laser are 1 V and 10 Gb/s, respectively. Therefore, an ultralow power consumption semiconductor light source will be a key device for on-chip optical interconnection systems.

Microdisk lasers [9] or photonic crystal lasers [10]–[12] have been reported to be promising devices for ultralow threshold operation because of their strong optical confinement structures; however, they have several disadvantages, such as low-output efficiency and high electrical resistance. Alternatively, we proposed a semiconductor membrane laser that utilizes a high-index contrast waveguide structure in the vertical direction. In the conventional laser structure, which has semiconductor cladding layers, the refractive index difference between the core region and the cladding region is about 5%, while an optical confinement factor of 1% per quantum well can be obtained from this structure. On the other hand, the proposed membrane structure consists of low-refractive index-material cladding layers, such as SiO_2 instead of a semiconductor. The membrane structure exhibits a large-refractive index difference—up to 40%—between the core region and the cladding region. In addition, the

Manuscript received December 1, 2010; revised January 31, 2011 and March 7, 2011; accepted March 10, 2011. Date of publication May 16, 2011; date of current version October 5, 2011. This work was supported in part by the Grants-in-Aid for Scientific Research from the Ministry of Education, Culture, Sports, Science, and Technology (MEXT), Japan, under Grant #19002009, Grant #22360138, Grant #21226010, Grant #08J55211, Grant #10J08973 and Grant #196860230, and in part by the Japan Society for the Promotion of Science (JSPS) FIRST Program. The work of T. Okumura was also supported by the Japan Society for the Promotion of Science (JSPS) for the Research Fellowship for Young Scientists.

T. Shindo, T. Okumura, H. Ito, T. Koguchi, D. Takahashi, Y. Atsumi, J. Kang, R. Osabe, T. Amemiya, and N. Nishiyama are with the Department of Electrical and Electronic Engineering, Tokyo Institute of Technology, Meguro-ku, Tokyo 152–8552, Japan (e-mail: shindou.t.aa@m.titech.ac.jp; tokumura@quantum.pe.titech.ac.jp; ito.h.ae@m.titech.ac.jp; koguchi.t.aa@m.titech.ac.jp; takahashi.d.aa@m.titech.ac.jp; atsumi.y.ab@m.titech.ac.jp; kang.j.aa@m.titech.ac.jp; osabe.r.aa@m.titech.ac.jp; amemiya.t.ab@m.titech.ac.jp; n-nishi@pe.titech.ac.jp).

S. Arai is with the Department of Electrical and Electronic Engineering and the Quantum Nanoelectronics Research Center, Tokyo Institute of Technology, Meguro-ku, Tokyo 152-8552, Japan (e-mail: arai@pe.titech.ac.jp).

Color versions of one or more of the figures in this paper are available online at http://ieeexplore.ieee.org.

Digital Object Identifier 10.1109/JSTQE.2011.2131636

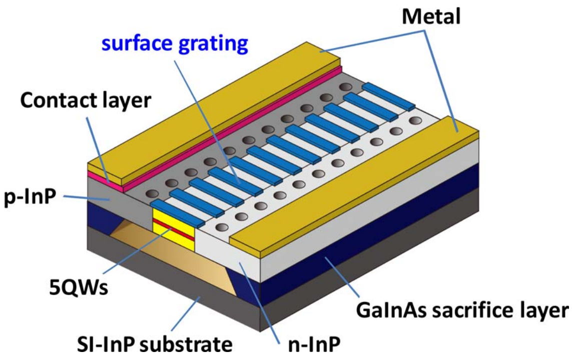

Fig. 1. LCI membrane DFB laser with air-bridge structure.

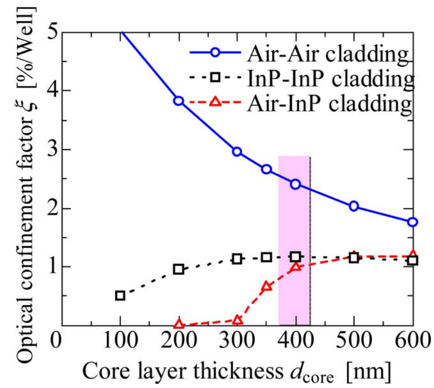

Fig. 2. Optical confinement factor as a function of the core layer thickness in various types of lasers.

membrane laser has a thin active layer (approximately 150 nm), which enhances the optical confinement factor to a value about three times higher than that of the conventional structure; consequently, it also enhances the modal gain at the same injection carrier density, and it leads to the realization of a short-cavity laser with threshold current less than 100 μA and with high-output efficiency. In previous works, an optically pumped semiconductor membrane laser with buried heterostructure consisting of a low-refractive index-material cladding layer of benzocyclobutene was demonstrated, and an optically pumped threshold power of $P_{\rm th} = 0.34$ mW was reported [13]. In this device, by introducing a wire-like active region to the DFB grating [14], the index-coupling coefficient κ_i was dramatically enhanced compared to that of the conventional structure. Furthermore, continuous wave (CW) operation temperatures up to 85 °C were realized [15]. In addition, a membrane laser with an air-bridge structure [16] and a membrane DFB laser bonded on a silicon-on-insulator substrate for silicon photonics integrated circuits were demonstrated [17], [18].

Our final target is ultralow threshold current operation of a current injection-type membrane DFB laser. Fig. 1 shows the expected structure of the current injection-type membrane DFB laser. Since the upper and lower cladding layers of the membrane laser are insulating materials or air, it is difficult to introduce a conventional vertical current injection structure. Therefore, we have been investigating methods to introduce a lateral-current-injection (LCI) structure formed by a two-step regrowth process [19]. As a step toward realizing the current injection-type membrane laser, we demonstrated a high-performance LCI-type Fabry–Perot (FP) laser with relatively thin core layers on a semi-insulating (SI) InP substrate [20]. However, to achieve a light source for on-chip optical interconnections, a DFB laser with a strongly coupled grating structure will be essential for meeting the requirements of low-power consumption and a small footprint. Therefore, we investigated the LCI-DFB laser with a surface grating structure prepared on an SI-InP substrate.

II. Theoretical Analysis and Device Design

We investigated the optimal core layer thickness and designed the grating structure for the LCI-DFB laser on an SI-InP substrate. First, we performed calculations to optimize the core layer thickness in the LCI-DFB laser prepared on an SI-InP substrate. Fig. 2 shows the calculated optical confinement factor ξ normalized by the number of quantum wells as a function of the core layer thickness $d_{\rm core}$ in three types of laser structures; we assumed that the active region consists of multiple quantum wells (MQWs) (6-nm-thick well and 9-nm-thick barrier) and that the number of MQWs is five. Data indicated by open squares correspond to those for the conventional semiconductor laser structure with thick InP cladding layers on both sides, and the data indicated by open triangles and open circles correspond to those for the LCI-DFB laser formed on an SI-InP substrate and for the LCI-DFB-type membrane structure with air cladding layers, respectively. The figure indicates that the membrane structure gives a higher optical confinement factor compared to that of the conventional laser structure, and the enhancement becomes larger as the core layer becomes thinner. When the core layer thickness of the membrane laser is less than 300 nm, the optical confinement factor can be enhanced to approximately three times that of the conventional structure. On the other hand, in the conventional laser and in the LCI-DFB laser on an SI-InP substrate, the optical confinement factor decreases as the core layer thickness decreases. This is especially true in the LCI-type laser on SI-InP; the optical confinement factor becomes almost zero when the core layer thickness is less than 300 nm because the optical field maxima exist in a much deeper position than that of the MQWs. Since the optical confinement factor of the LCI-DFB laser on an SI-InP substrate is almost the same as that of the conventional-type lasers for core layer thicknesses of about 400 nm, we choose 400 nm for the calculation and fabrication of the LCI-DFB laser on an SI-InP substrate.

Next we designed the surface grating structure from the viewpoint of the optical confinement factor of the active region (5QWs) and the index-coupling coefficient. As previous study, we demonstrated the LCI-DFB laser with a GaInAsP etched surface grating structure in which we partially etched the GaInAsP layer from the top surface of the initial wafer, as shown in Fig. 3(a) [21]. A simple fabrication process is the advantage of the directly etched surface grating structure. Then, in this device, we realized an operation of the LCI-DFB laser under a pulse current condition. But an operation under a CW condition was not realized in the device. Fig. 3(b) shows the grating depth

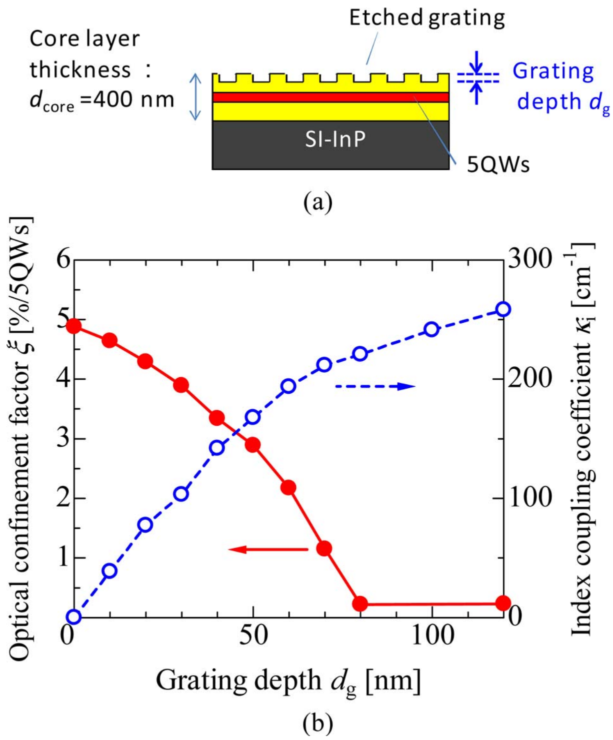

Fig. 3. (a) Calculated structure and (b) optical confinement factor in the grooved region (indicated by a solid line) and index-coupling coefficient (indicated by a dashed line) as a function of the etched grating depth.

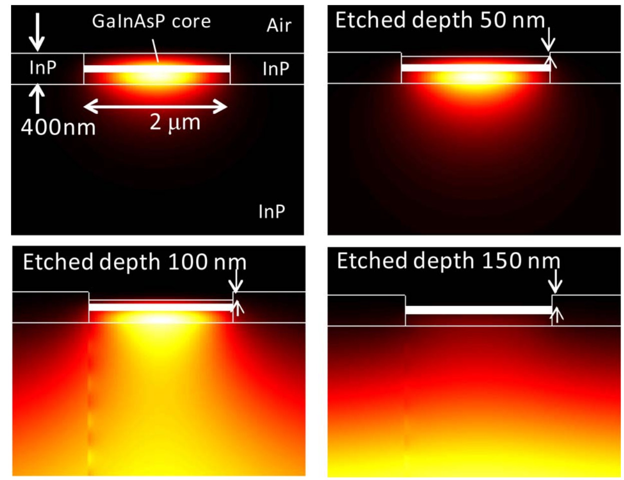

Fig. 4. Cross-sectional optical mode field of the LCI-DFB laser with various etching depths.

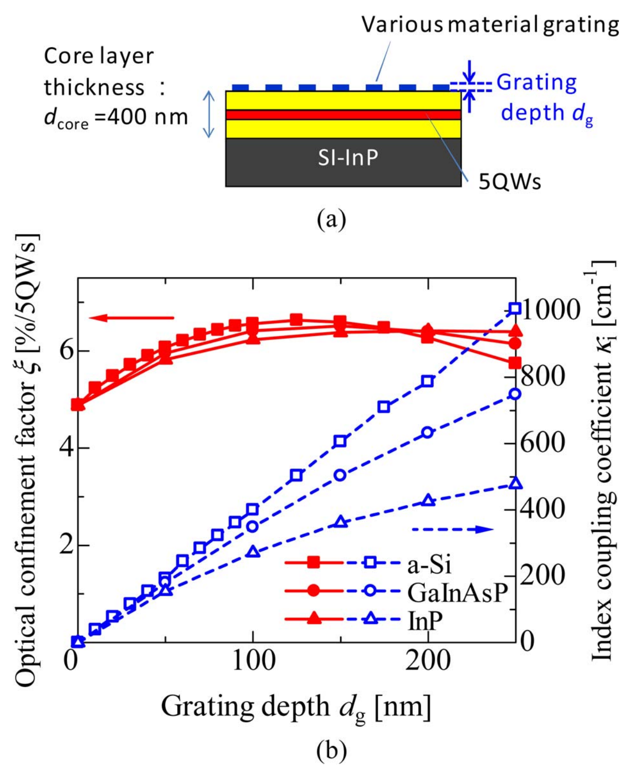

Fig. 5. (a) Calculated structure and (b) optical confinement factor in the grooved region (indicated by a solid line) and index-coupling coefficient (indicated by a dashed line) as a function of the various materials' grating depth.

dependences of the optical confinement factor and the index-coupling coefficient for the LCI-DFB laser with the etched surface grating, where the core layer thickness and the stripe width W_S were assumed to be 400 nm and 2.0 μm, respectively, and the grating was assumed to be rectangular in shape with a duty ratio of 1/2 and the optical confinement factor was calculated for the grooved region. The refractive index of the GaInAsP optical confinement layer (OCL) was assumed to be 3.34. As can be seen, the optical confinement factor steeply decreases with an increase of the etching depth, and the index-coupling coefficient bends downward from the initial slope to about 250 cm^{-1} when the grating depth d_g is 120 nm. Fig. 4 indicates the optical mode field of the LCI-DFB laser for various etched depths. As can be seen, the optical mode field is confined in the stripe region for d_g up to 50 nm, and it becomes leaky for $d_g = 150$ nm; thus, the increase in the etched grating depth reduces the optical confinement factor and increases the waveguide loss of the LCI-DFB laser. Consequently, it is difficult to realize a high index-coupling coefficient together with a high optical confinement in this waveguide structure with a core layer thickness of less than 300 nm, as indicated by the triangles in Fig. 2.

Fig. 5(b) shows the optical confinement factor in the grooved region and the index-coupling coefficient as a function of the grating depth. In this calculation, we designed the surface grating with various materials such as amorphous-Si (a-Si), GaInAsP, and InP. The core layer thickness and the stripe width were again assumed to be 400 nm and 2.0 μm, respectively. In this surface grating, the surface grating will be formed by depositing another material on the core layer. The refractive indices of a-Si, GaInAsP, and InP were assumed to be 3.45, 3.34, and 3.17, respectively. As can be seen in Fig. 5(b), the optical confinement factor of these surface gratings can be increased for various grating depths compared with that of the etched surface structure as shown in Fig. 3(b) because the thickness of the core layer is sufficient to support the guided mode. Fig. 6 shows the calculated cross-sectional optical mode field of the LCI-DFB laser with the a-Si surface grating. It can be confirmed that the optical confinement factor becomes much more stable for various a-Si grating depths compared with that

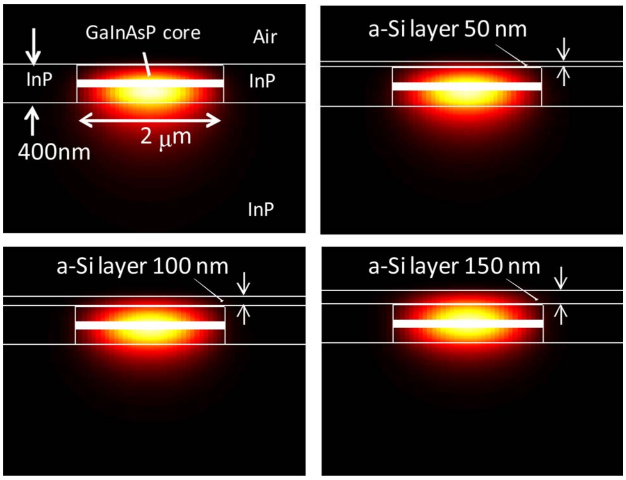

Fig. 6. Cross-sectional optical mode field of the LCI-DFB laser with a-Si surface grating with various grating depths.

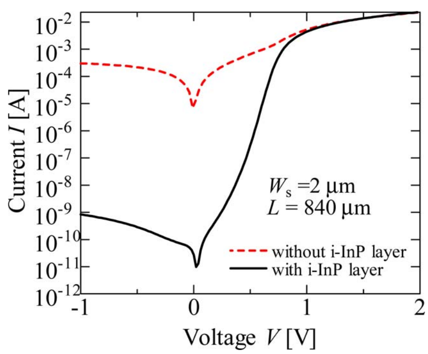

Fig. 7. *V–I* characteristics of the LCI-FP laser.

of the etched surface grating structure (see Fig. 4). The index-coupling coefficient of the a-Si surface grating is larger than that of the GaInAsP surface grating and InP surface grating due to its large refractive-index difference between the a-Si layer and air. In addition, since the a-Si layer can be deposited after the formation of the LCI structure, it can be applied to the LCI-DFB laser without a significant change in the fabrication process and the initial wafer structure. So, by introducing the a-Si surface grating, it is possible to improve the lasing characteristics due to its high optical confinement factor and high index-coupling coefficient.

In addition to the unstable optical mode field (see Fig. 4), the surface recombination in the exposed GaInAsP layer was expected to be the cause of the poor lasing properties in the LCI-DFB laser with etched surface grating [21] since the surface recombination speed of GaInAsP is about one order of magnitude larger than that of InP [22]. In the LCI-DFB laser with the a-Si surface grating, a thin i-InP layer was introduced under the a-Si layer to prevent exposure of the upper GaInAsP OCL which has high surface recombination speed. First, we confirmed the effect of introducing the i-InP layer to prevent exposure of the upper GaInAsP OCL. Fig. 7 shows the *V–I* characteristics of the LCI structure. The solid line shows the *V–I* characteristic of the LCI structure with a 10 nm i-InP layer on the GaInAsP core layer, and the dashed line shows that of the same device after removal of the i-InP layer by the CH_4/H_2 dry etching process. Large carrier leakage was observed from the *V–I* characteristics of the LCI-FP laser without the i-InP layer. The nonradiative surface recombination in the exposed upper OCL was attributed to this large carrier leakage. Therefore, by introducing the a-Si surface grating on the i-InP layer, it is possible to improve the lasing characteristics as compared to that of the LCI-FP laser with etched surface grating [21].

III. Fabrication Process

In the LCI-DFB laser with an a-Si surface grating structure on an SI-InP substrate, an initial wafer with an undoped GaInAsP core layer—which consisted of a lower OCL ($\lambda_g = 1.2\ \mu$m, 140 nm thick), 1% compressive-strained $Ga_{0.22}In_{0.78}As_{0.81}P_{0.19}$ 5 quantum wells (6 nm thick), 0.15% tensile-strained barriers (10 nm), an upper OCL ($\lambda_g = 1.2\ \mu$m, 140 nm thick), and an undoped thin (10 nm) InP layer—was grown by organometallic vapor phase epitaxy (OMVPE) on an Fe-doped SI-InP substrate. The total GaInAsP core layer thickness was about 360 nm so that the optical confinement factor of the active layer would be almost the same as that of a conventional double heterostructure with thick cladding layers.

First, the LCI structure was fabricated by CH_4/H_2 RIE and two-step OMVPE selective area growth. Mesa structures with a width of 7 μm and a height of 400 nm were formed with a SiO_2 mask and the CH_4/H_2 RIE process. After removing the damaged surfaces due to dry etching by wet chemical cleaning, n-InP ($N_d = 4 \times 10^{18}$/cm^3) was selectively regrown on both sides of the mesa structure as cladding layers. Next, by etching a part of the wide mesa structure and one side of the embedded n-type layer in a similar manner, narrow (2-μm-wide) stripes were formed so as to achieve fundamental transverse mode operation. Then, p-InP ($N_d = 4 \times 10^{18}$/cm^3) and p-GaInAs ($N_d = 8 \times 10^{18}$/cm^3) were regrown in the same way, and the part of the GaInAs contact layer near the stripe edge was removed by wet chemical etching to reduce optical absorption. Next, Ti/Au electrodes were evaporated onto the p-contact and the n-InP sections, and a lift-off process was carried out for the contact pad. Then, the surface grating structure was formed by electron beam lithography (EBL) and the dry etching process. After deposition of the a-SI layer (30 nm) and spin coating of EB resist (ZEP520 mixed with C_{60}), 10-μm-wide surface grating patterns were formed by EBL. Next, CF_4 inductively coupled plasma (ICP) etching was carried out to etch the grating pattern. Please note that the negligible absorption of our a-Si film has been confirmed by fabricating low-loss a-Si wire waveguides [23]. Finally, the unnecessary a-Si layer on the electrodes was removed by a CF_4 RIE process.

IV. Experimental Results

The schematic structure of the fabricated LCI-DFB laser with the a-Si surface grating is shown in Fig. 8. As can be seen, the a-Si layer was deposited on the i-InP layer. Fig. 9 shows top and cross-sectional SEM views of the fabricated LCI-DFB laser with the a-Si surface grating which was formed on the top of

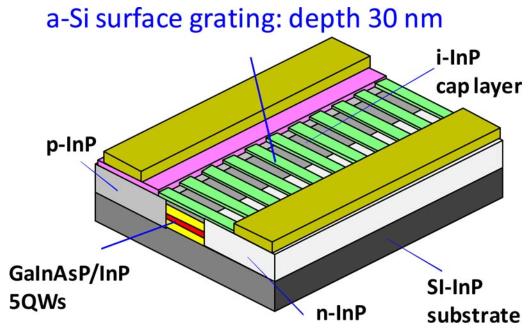

Fig. 8. Schematic device structure of the LCI-DFB laser with a-Si surface grating.

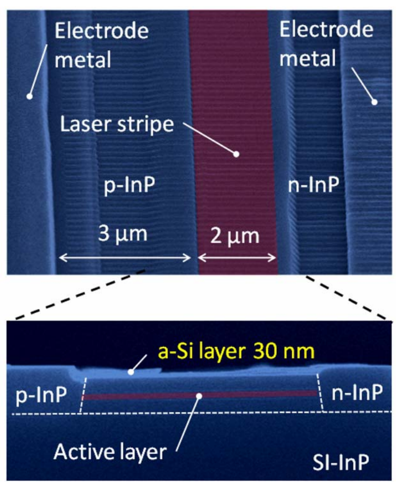

Fig. 9. SEM view of the LCI-DFB laser with a-Si surface grating.

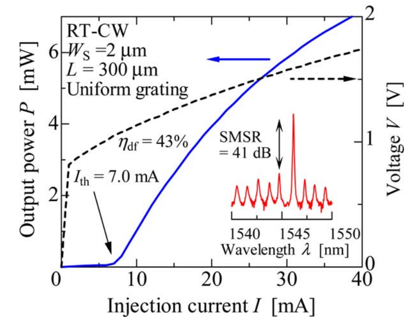

Fig. 10. *I–L* and *I–V* curves of the fabricated LCI-DFB laser with a-Si uniform surface grating.

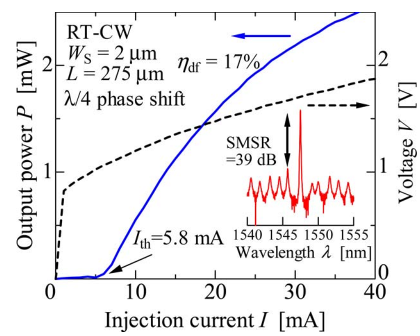

Fig. 11. *I–L* and *I–V* curves of the fabricated LCI-DFB laser with a-Si λ/4 phase-shifted surface grating.

the laser stripe. The total core thickness was about 360 nm. The a-Si grating period and the depth were 243.75 and 30 nm, respectively. The index-coupling coefficient estimated from the calculation result [see Fig. 5(b)] was about 100 cm^{-1}. In addition, the interspaces between the laser stripe and the electrode metal in p-doped InP region was set to 3 μm.

Fig. 10 shows the *I–L* (solid line) and *V–I* (dashed line) characteristics of the LCI-DFB laser with the a-Si surface grating under an RT-CW condition. The cavity length and the stripe width were 300 and 2.0 μm, respectively. Hence, the grating coupling strength $\kappa_i L$ was estimated to be around 3.0. A low $I_{\rm th}$ of 7.0 mA and a high differential quantum efficiency from the front facet $\eta_{\rm df}$ of 43% were obtained. This value represents the highest differential quantum efficiency from a single facet ever reported for LCI-type lasers. The differential series resistance and the voltage at the threshold current were around 25 Ω and 1.1 V, respectively. The series resistance depends mainly on the resistance of the p-doped InP region which has high sheet resistance [24]. By reduction of the interspace between the laser stripe and the electrode metal in the p-doped InP region, a lower series resistance can be attained.

The inset of Fig. 10 shows the lasing spectrum at a bias current twice the threshold current (I = 14.0 mA). As can be seen, a lasing wavelength of 1546 nm and an SMSR of 41 dB were obtained. Because the index-coupling coefficient was not higher than that of previously reported DFB lasers with wire-like active regions [14], a clear stopband was not observed, but a resonant mode spacing of about 1 nm was observed, and this corresponds to FP resonance at a cavity length of 300 μm.

Fig. 11 shows the lasing characteristics of a λ/4 phase-shifted LCI-DFB laser with the a-Si surface grating. The cavity length and the stripe width were 275 and 2.0 μm, respectively. The λ/4 phase shift was introduced at 130 μm from the front facet in DFB cavity. A threshold current $I_{\rm th}$ of 5.8 mA and a differential quantum efficiency η_d of 17% from the front facet were obtained. This threshold current was the lowest value ever reported in LCI-type lasers. The inset of Fig. 9 shows the lasing spectrum at a bias current twice the threshold current (I = 12 mA). A single-mode operation and phase-shifted mode oscillation were obtained from this figure.

Finally, the dynamic characteristics of the uniform grating LCI-DFB laser with the a-Si surface grating (see Fig. 10) were measured after bonding on an AlN coplanar submount with a 40 Ω matching resistance for high-speed measurements. First, we measured the dependence of the relaxation oscillation frequency f_r on the square root of the bias current above the threshold $(I - I_{\rm th})^{1/2}$ as the peak frequency of the relative intensity noise spectrum. Then, a modulation current efficiency factor (MCEF) of approximately 1.0 GHz/mA$^{1/2}$ was obtained. This value is at least twice those of previously reported LCI-FP lasers [25]. Fig. 12 shows the small-signal modulation response S_{21} of this laser as measured by a network analyzer. In this measurement, the bias current applied to the laser was varied from 10 to 30 mA. A small-signal modulation bandwidth of 4.8 GHz

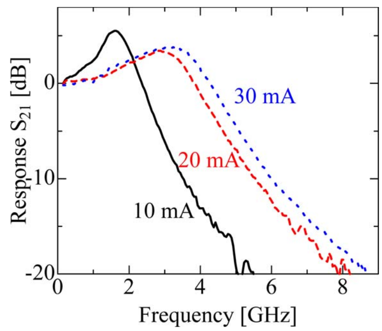

Fig. 12. Small-signal modulation response of the LCI-DFB laser with a-Si surface grating.

was obtained at a bias current of 30 mA. This bandwidth may be attributed to the higher internal quantum efficiency and shorter cavity length as compared to those of previously reported LCI-FP lasers [24]. By introducing a high index-coupling grating structure with wire-like active regions to the proposed laser, a much higher MCEF can be expected [26], [27].

V. Conclusion

In conclusion, we demonstrated LCI-type DFB lasers with a surface grating structure prepared on an SI-InP substrate. First, we designed and optimized the device structure to realize the surface grating structure, which has a high index-coupling coefficient together with a high optical confinement in quantum wells, and adopted a sufficiently thick (400 nm) GaInAsP core layer and a-Si surface grating prepared on an SI-InP substrate. We obtained operation that was characterized by moderately low threshold current and high differential quantum efficiency. From the measurement result of the LCI-DFB laser with a-Si uniform grating, a threshold current of $I_{\rm th} = 7.0$ mA and an external differential quantum efficiency from the front facet of $\eta_{\rm df} = 43\%$ were achieved under RT-CW conditions with a stripe width of 2.0 μm and a cavity length of 300 μm. In a λ/4 phase-shifted LCI-DFB laser with the a-Si surface grating, we obtained the lowest threshold current of 5.8 mA ever reported in LCI-type lasers. Furthermore, from a small-signal response, the bandwidth of 4.8 GHz at a bias current of 30 mA of the LCI-DFB laser with the a-Si uniform grating was realized. These results indicate that this LCI-DFB structure can be applied to realize low-power consumption lasers based on a membrane structure with a high-index contrast waveguide.

Acknowledgment

The authors would like to thank Prof. E. Y. Suematsu and Prof. K. Iga for their continuous encouragement and Prof. M. Asada, Prof. F. Koyama, Prof. T. Mizumoto, Prof. Y. Miyamoto, and Dr. S. Lee, Tokyo Institute of Technology, for fruitful discussions. The first author would like to acknowledge the JSPS for the Research Fellowship for Young Scientists.

References

[1] P. Kapur, J. P. McVittie, and K. C. Saraswat, "Technology and reliability constrained future copper interconnects—Part I: Resistance modeling," *IEEE Trans. Electron Devices*, vol. 49, no. 4, pp. 590–597, Apr. 2002.

[2] P. Kapur, G. Chandra, J. P. McVittie, and K. C. Saraswat, "Technology and reliability constrained future copper interconnects—Part II: Performance implications," *IEEE Trans. Electron Devices*, vol. 49, no. 4, pp. 598–604, Apr. 2002.

[3] S. List, M. Bamal, M. Stucchi, and K. Maex, "A global view of interconnects," *Microelectron. Eng.*, vol. 83, no. 11–12, pp. 2200–2207, Nov. 2006.

[4] D. A. B. Miller, "Rationale and challenges for optical interconnects to electronic chips," *Proc. IEEE*, vol. 88, no. 6, pp. 728–749, Jun. 2000.

[5] G. Chen, H. Chen, M. Haurylau, N. A. Nelson, D. H. Albonesi, P. M. Fauchet, and E. G. Friedman, "Prediction of CMOS compatible on-chip optical interconnect," *Integrat. VLSI J.*, vol. 40, no. 4, pp. 434–446, Oct. 2006.

[6] D. Liang, M Fiorentino, T. Okumura, H. H. Chang, D. T. Spencer, Y. H. Kuo, A. W. Fang, D. Dai, R. G. Beausoleil, and J. E. Bowers, "Electrically-pumped compact hybrid silicon microring lasers for optical interconnects," *Opt. Express*, vol. 17, no. 22, pp. 20355–20364, Oct. 2009.

[7] R. Nagarajan, M. Kato, J. Pleumeekers, P. Evans, D. Lambert, A. Chen, V. Dominic, A. Mathur, P. Chavarkar, M. Missey, A. Dentai, S. Hurtt, J. Back, R. Muthiah, S. Murthy, R. Salvatore, S. Grubb, C. Joyner, J. Rossi, R. Schneider, M. Ziari, F. Kish, and D. Welch, "Single-chip 40-channel InP transmitter photonic integrated circuit capable of aggregate data rate of 1.6 Tbit/s," *Electron. Lett.*, vol. 42, no. 22, pp. 771–772, Jun. 2006.

[8] D. A. B. Miller, "Device requirements of optical interconnects to silicon chips," *Proc. IEEE*, vol. 97, no. 7, pp. 1166–1185, Jul. 2009.

[9] M. Fujita, R. Ushigome, and T. Baba, "Continuous wave lasing in GaInAsP microdisk injection laser with threshold current of 40 μA," *Electron. Lett.*, vol. 36, no. 9, pp. 790–791, Apr. 2000.

[10] O. Painter, R. K. Lee, A. Scherer, A. Yariv, J. D. O'Brien, P. D. Dapkus, and I. Kim, "Two-dimensional photonic band-gap defect mode laser," *Science*, vol. 284, no. 11, pp. 1819–1821, Jun. 1999.

[11] H. G. Park, S. H. Kim, S. H. Kwon, Y. G. Ju, J. K. Yang, J. H. Beak, S. B. Kim, and Y. H. Lee, "Electrically driven single-cell photonic crystal laser," *Science*, vol. 305, no. 5689, pp. 1444–1447, Sep. 2004.

[12] C. Seassal, C. Monat, J. Mouette, E. Touraille, B. B. Bakir, H. T. Hattori, J. L. Leclercq, X. Letartre, P. R. Romeo, and P. Viktorovitch, "InP-bonded membrane photonic components and circuits: Toward 2.5 dimensional micro-nano-photonics," *IEEE J. Sel. Top. Quantum Electron.*, vol. 11, no. 2, pp. 395–407, Mar 2005.

[13] S. Sakamoto, H. Naitoh, M. Otake, Y. Nishimoto, S. Tamura, T. Maruyama, N. Nishiyama, and S. Arai, "Strongly index-coupled membrane BH–DFB lasers with surface corrugation grating," *IEEE J. Sel. Top. Quantum Electron.*, vol. 13, no. 5, pp. 1135–1141, Sep./Oct. 2007.

[14] N. Nunoya, M. Nakamura, M. Morshed, S. Tamura, and S. Arai, "High-performance 1.55-μm wavelength GaInAsP-InP distributed-feedback lasers with wirelike active regions," *IEEE J. Sel. Top. Quantum Electron.*, vol. 7, no. 2, pp. 249–258, Jun. 2001.

[15] S. Sakamoto, H. Naitoh, M. Ohtake, Y. Nishimoto, T. Maruyama, N. Nishiyama, and S. Arai, "85 °C continuous-wave operation of GaInAsP/InP-membrane buried heterostructure distributed feedback lasers with polymer cladding layer," *Jpn. J. Appl. Phys.*, vol. 46, no. 47, pp. L1155–L1157, 2007.

[16] H. Naitoh, S. Sakamoto, M. Ohtake, T. Okumura, T. Maruyama, N. Nishiyama, and S. Arai, "GaInAsP/InP membrane BH–DFB laser with air-bridge structure," *Jpn. J. Appl. Phys.*, vol. 46, no. 47, pp. 1158–1160, Nov. 2007.

[17] T. Maruyama, T. Okumura, S. Sakamoto, K. Miura, Y. Nishimoto, and S. Arai, "GaInAsP/InP membrane BH–DFB lasers directly bonded on SOI substrate," *Opt. Express*, vol. 14, no. 18, pp. 8184–8188, Sep. 2006.

[18] T. Okumura, T. Maruyama, M. Kanemaru, S. Sakamoto, and S. Arai, "Single-mode operation of GaInAsP/InP-membrane distributed feedback lasers bonded on silicon-on-insulator substrate with rib-waveguide structure," *Jpn. J. Appl. Phys.*, vol. 46, no. 48, pp. 1206–1208, Dec. 2007.

[19] K. Oe, Y. Noguchi, and C. Caneau, "GaInAsP lateral current injection lasers on semiinsulating substrates," *IEEE Photon. Technol. Lett.*, vol. 6, no. 4, pp. 479–481, Apr. 1994.

[20] T. Okumura, M. Kurokawa, M. Shirao, D. Kondo, H. Ito, N. Nishiyama, T. Maruyama, and S. Arai, "Lateral current injection GaInAsP/InP laser

on semiinsulating substrate for membrane-based photonic circuits," *Opt. Express*, vol. 17, no. 15, pp. 12564–12570, Jul. 2009.

[21] T. Okumura, M. Kurokawa, D. Kondo, H. Ito, N. Nishiyama, and S. Arai, "Lateral current injection type GaInAsP/InP DFB lasers on SI–InP substrate," in *Proc. IEEE 21st Int. Conf. Indium Phosphide and Related Mater.*, Newport Beach, CA, May 2009, p. 178, Paper TuB2.

[22] S. Sakai, M. Umeno, and Y. Amemiya, "Measurement of diffusion coefficient and surface recombination velocity for p-InGaAsP grown on InP," *Jpn. J. Appl. Phys.*, vol. 19, no. 1, pp. 109–113, Jan. 1980.

[23] J. Kang, K. Inoue, Y. Atsumi, N. Nishiyama, and S. Arai, "Loss measurement of multiple layer a-Si waveguides," presented at the Int. Conf. Solid State Devices and Mater., Tokyo, Japan, Sep. 2010, Paper D-8-2.

[24] T. Okumura, H. Ito, D. Kondo, N. Nishiyama, and S. Arai, "Continuous wave operation of thin film lateral current injection lasers grown on semi-insulating InP," *Jpn. J. Appl. Phys.*, vol. 49, no. 4, pp. 040205-1–040205-3, Apr. 2010.

[25] T. Okumura, D. Kondo, H. Ito, S. Lee, D. Takahashi, N. Nishiyama, and S. Arai, "Dynamic characteristics of lateral current injection laser," presented at 37th International Symposium Compound Semiconductor, Takamatsu, Japan, Jun. 2010, Paper WeE3-2.

[26] K. Ohira, N. Nunoya, and S. Arai, "Stable single-mode operation of distributed feedback lasers with wirelike active regions," *IEEE J. Sel. Top. Quantum Electron.*, vol. 9, no. 5, pp. 1166–1171, Sep./Oct. 2003.

[27] T. Shindo, S. Lee, D. Takahashi, N. Tajima, N. Nishiyama, and S. Arai, "Low-threshold and high-efficiency operation of distributed reflector laser with wirelike active regions," *IEEE Photon. Technol. Lett.*, vol. 21, no. 19, pp. 1414–1416, Oct. 2009.

Takahiko Shindo (S'10) received the B.E. and M.E. degrees from Tokyo Institute of Technology, Meguro-ku, Tokyo, Japan, in 2008 and 2010, respectively, both in electrical and electronic engineering. He is currently working toward the Ph.D. degree at the Quantum Electronics Research Center (QNERC), Tokyo Institute of Technology.

From 2010, he has also been a Research Fellow in the Japan Society for the Promotion of Science (JSPS), Japan. His current research interests include photonic integrated devices on a silicon platform.

Mr. Shindo is a student member of the Japan Society of Applied Physics.

Tadashi Okumura (S'08–M'10) was born in Gifu Prefecture, Japan, in 1983. He received the B.E., M.E. and Ph.D. degrees from the Tokyo Institute of Technology, Meguro-ku, Tokyo, Japan, in 2006, 2008, and 2010, respectively.

In 2009, he joined the University of California-Santa Barbara as a Visiting Scholar. His research interests include silicon photonics and membrane-based photonic devices for optical interconnection.

Dr. Okumura is a member of the Japan Society of Applied Physics. He received a Research Fellow for Young Scientists in the Japan Society for the Promotion of Science (JSPS), Japan.

Hitomi Ito received the B.E. and M.E. degrees from Tokyo Institute of Technology, Meguro-ku, Tokyo, Japan, in 2009 and 2011, respectively, both in electrical and electronic engineering.

She is a member of the Japan Society of Applied Physics.

Takayuki Koguchi was born in Tochigi Prefecture, Japan, in 1988. He received the B.E. degree in electrical and electronic engineering from the Tokyo Institute of Technology, Meguro-ku, Tokyo, Japan, in 2010, where he is currently working toward the M.E. degree in the Department of Electrical and Electronic Engineering, Tokyo Institute of Technology.

His current research interests include hybrid photonic integrated circuits.

Mr. Koguchi is a member of the Japan Society of Applied Physics.

Daisuke Takahashi (S'11) was born in Kanagawa Prefecture, Japan, in 1986. He received the B.E. and M.E. degrees in electrical and electronic engineering from the Tokyo Institute of Technology, Meguro-ku, Tokyo, Japan, in 2009 and 2011, respectively.

His current research interests include high-speed semiconductor lasers for future access networks.

Mr. Takahashi is a student member of the Japan Society of Applied Physics, Institute of Electrical, Information and Communication Engineers (IEICE), and IEEE Photonics Society.

Yuki Atsumi (S'09) was born in Aichi Prefecture, Japan, in 1986. He received the B.E. and M.E. degrees in electrical and electronic engineering from Tokyo Institute of Technology, Meguro-ku, Tokyo, Japan, in 2009 and 2011, respectively. He is currently working toward the Ph.D. degree in the Department of Electrical and Electronic Engineering, Tokyo Institute of Technology.

Since 2011, he has also been a Research Fellow at the Japan Society for the Promotion of Science, Japan. His current research interests include athermal photonic integrated devices on a silicon platform.

Mr. Atsumi is a member of the Japan Society of Applied Physics.

Joonhyun Kang was born in Seoul, Korea, in 1986. He received the B.E. degrees in electrical and electronic engineering from Tokyo Institute of Technology, Meguro-ku, Tokyo, Japan, in 2010.

His current research interests include 3-D a-Si optical circuits.

Mr. Kang is a member of the Japan Society of Applied Physics.

Ryo Osabe was born in Niigata Prefecture, Japan, in 1988. He received the B.E. degree in electrical and electronic engineering from Tokyo Institute of Technology, Meguro-ku, Tokyo, Japan, in 2010, where he is currently working toward the M.E. degree in the Department of Electrical and Electronic Engineering.

His current research interests include hybrid photonic integrated circuits.

Mr. Osabe is a member of the Japan Society of Applied Physics.

Tomohiro Amemiya (S'06–M'09) received the B.S., M.S., and Ph.D. degrees from the University of Tokyo, Bunkyo, Tokyo, Japan, in 2004, 2006, and 2009, respectively, all in electronic engineering.

In 2009, he joined the Quantum Electronics Research Center, Tokyo Institute of Technology, Meguro-ku, Tokyo, Japan, where he is currently an Assistant Professor. His research interests include physics of semiconductor light-controlling devices, metamaterials for optical frequency, magnetooptical devices, and in the processing technologies for fabricate these devices.

Dr. Amemiya is a member of the Optical Society of America, the American Physical Society, and the Japan Society of Applied Physics. He was the recipient of the 2007 IEEE Photonics Society Annual Student Paper Award and the 2008 IEEE Photonics Society Graduate Student Fellowships.

Nobuhiko Nishiyama (M'01–SM'07) was born in Yamaguchi Prefecture, Japan, in 1974. He received the B.E., M.E., and Ph.D. degrees from the Tokyo Institute of Technology, Meguro-ku, Tokyo, Japan, in 1997, 1999, and 2001, respectively. During the Ph.D. study, he demonstrated single-mode 0.98 and 1.1 μm vertical cavity surface emitting laser (VCSEL) arrays with stable polarization using misoriented substrates for high-speed optical networks as well as MOCVD-grown GaInNAs VCSELs.

He joined Corning, Inc., NY, in 2001 and worked with the Semiconductor Technology Research Group. At Corning, Inc., he was engaged on several subjects including short-wavelength lasers, 1060-nm DFB/DBR lasers, and long-wavelength InP-based VCSELs, demonstrating state-of-the-art results such as 10-Gb/s isolator-free and high-temperature operations of long-wavelength VCSELs. Since 2006, he has been an Associate Professor at the Tokyo Institute of Technology. His current research interests include laser transistors, silicon-photonics, III–V silicon hybrid optical devices, and terahertz-optical signal conversions involving optics–electronics–radio integration circuits.

Dr. Nishiyama received the Excellent Paper Award from the Institute of Electronics, Information and Communication Engineers (IEICE) of Japan in 2001 and the Young Scientists Prize in the Commendation for Science and Technology from the Minister of Education, Culture, Sports, Science and Technology in 2009. He is a member of the Japan Society of Applied Physics, IEICE, and IEEE Photonics Society.

Shigehisa Arai (M'83–SM'06–F'10) was born in Kanagawa Prefecture, Japan, in 1953. He received the B.E., M.E., and D.E. degrees from Tokyo Institute of Technology, Meguro-ku, Tokyo, Japan, in 1977, 1979, and 1982, respectively, all in electronics. During the Ph.D. study, he demonstrated room-temperature CW operations of 1.11–1.67 μm long-wavelength lasers fabricated by a liquid-phase-epitaxy as well as their single-mode operations under a rapid direct modulation.

He joined the Department of Physical Electronics, Tokyo Institute of Technology, as a Research Associate in 1982, and joined AT&T Bell Laboratories, Holmdel, NJ, as a Visiting Researcher from 1983 to 1984, on leave from Tokyo Institute of Technology. Then, he became a Lecturer in 1984, an Associate Professor in 1987, and a Professor with the Research Center for Quantum Effect Electronics and the Department of Electrical and Electronic Engineering in 1994. Since 2004, he has been a Professor with the Quantum Nanoelectronics Research Center, Tokyo Institute of Technology. His research interests include photonic integrated devices such as dynamic-single-mode and wavelength-tunable semiconductor lasers, semiconductor optical amplifiers, and optical switches/modulators. His current research interests include studies on low-damage and cost-effective processing technologies of ultrafine structures for high-performance lasers and photonic integrated circuits on silicon platforms.

Dr. Arai is a member of the Optical Society of America, the Institute of Electronics, Information and Communication Engineers (IEICE), and the Japan Society of Applied Physics (JSAP). He received the Excellent Paper Award from the IEICE of Japan, in 1988, the Michael Lunn Memorial Award from the Indium Phosphide and Related Materials Conference in 2000, prizes for science and technology including the Commendation for Science and Technology from the Minister of Education, Culture, Sports, Science and Technology in 2008, the Electronics Society Award from the IEICE in 2008, and the JSAP Fellowship in 2008.